

Membrane Properties of Neuron-Like Cells Generated from Adult Human Bone-Marrow-Derived Mesenchymal Stem Cells

Lyle E. Fox,¹ Jun Shen,¹ Ke Ma,² Qing Liu,¹ Guangbin Shi,² George D. Pappas,² Tingyu Qu,² and Jianguo Cheng¹

Adult mesenchymal stem cells (MeSCs) isolated from human bone marrow are capable of generating neural stem cell (NSC)-like cells that can be subsequently differentiated into cells expressing molecular markers for neurons. Here we report that these neuron-like cells had functional properties similar to those of brain-derived neurons. Whole-cell patch-clamp recordings and calcium imaging experiments were performed on neuron-like cells differentiated from bone-marrow-derived NSC-like cells. The neuron-like cells were subjected to current pulses to determine if they were capable of generating depolarization-induced action potentials. We found that nearly all of the cells with neuron-like morphology exhibited active membrane properties in response to the depolarizing pulses. The most common response was a single spike-like event with an overshoot and brief afterhyperpolarization. Cells that did not generate overshooting spike-like events usually displayed rectifying current-voltage relationships. The prevalence of these active membrane properties in response to the depolarizing current pulses suggested that the human MeSCs (hMeSCs) were capable of converting to a neural lineage under defined culture conditions. The spike-like events were blocked by the voltage-gated sodium channel inhibitor lidocaine, but unaffected by another sodium channel inhibitor tetrodotoxin (TTX). In calcium imaging experiments, the neuron-like cells responded to potassium chloride depolarization and L-glutamate application with increases in the cytoplasmic calcium levels. Thus, the neuron-like cells appeared to express TTX-resistant voltage-gated sodium channels, voltage-gated calcium channels, and functional L-glutamate receptors. These results demonstrate that hMeSCs were capable of generating cells with characteristics typical of functional neurons that may prove useful for neuroreplacement therapies.

Introduction

TRANSPLANTATION OF HUMAN embryonic stem cells is considered a promising therapy for traumatic injuries and degenerative diseases because stem cells have the potential to develop into and replace many different types of tissue, including those with a limited capacity for self-repair like the central nervous system (CNS). Yet, technical difficulties isolating neural stem cells (NSCs) and ethical concerns, among other issues, have limited the use of embryonic stem cells in clinical settings [1,2]. For example, transplanted embryonic stem cells can cause immune reactions and tumors that can damage healthy tissue [3–5]. In addition, the techniques that are traditionally used to grow and differentiate embryonic stem cells for therapeutic applications, cocultures with feeder cells, and/or a medium containing animal products are potentially harmful [1]. The ideal stem

cell for clinical use would be isolated from the patient's own tissue.

Adult stem cells, like human mesenchymal stem cells (hMeSCs), may reduce some of the controversial ethical issues and technical problems associated with the use of embryonic stem cells. The hMeSCs are relatively easy to isolate from the bone marrow (BM) and also grow well in culture. The hMeSCs are self-renewable multipotent stem cells capable of differentiating into various mesenchymal lineages, including osteogenic, chondrogenic, adipogenic, and fibroblastic cells [6–8]. Several recent studies have shown that hMeSCs are also capable of being directly induced into neuron- and glia-like cells under experimentally defined culture conditions [9–16] and after transplantation into the CNS [15,17,18]. This direct induction of MeSCs to differentiate into neuronal- and glial-like phenotypes usually involves exposure to growth factors, potentially toxic chemical

¹Department of Pain Management, Cleveland Clinic Foundation, Cleveland, Ohio.

²Department of Psychiatry, The Psychiatric Institute, College of Medicine, University of Illinois at Chicago (UIC), Chicago, Illinois.

agents, and cocultures with neural cells. In addition, the survival of terminally differentiated neuron- and glia-like cells after transplantation into the CNS is often poor [1,19]. The survival of undifferentiated embryonic stem cells is better, but very few differentiate into neurons that integrate into the brain or spinal cord, and the risk for tumor formation increases [17,20–23].

The BM-derived hMeSCs can be converted into NSC-like cells that can subsequently differentiate into neuron- and glia-like cells in culture [13,14,24,25]. Recently, we succeeded in generating NSC-like cells by cultivating the isolated hMeSCs in a conditioned medium of human neural stem cells (hNSCs-CM) without using a coculture system, chemical treatment, or genetic modification. After culturing in a serum-free differentiation medium, these NSC-like cells further developed into glia-like cells expressing a marker for astrocytes, glial fibrillary acidic protein (GFAP), and neuron-like cells expressing the neuronal markers, microtubule-associated protein 2 (MAP₂), β III-tubulin, neurofilament 200 (NF-200), gamma aminobutyric acid (GABA), and glutamate. Although these cells have the morphological and immunocytochemical characteristics of neurons, little is known about their functional properties. We used patch clamp recording to determine if the neuron-like cells were capable of generating an action potential in response to depolarizing current pulses and calcium imaging to ascertain if they expressed voltage-gated calcium channels and neurotransmitter receptors. Electrophysiological analyses demonstrated that the neuron-like cells differentiated from the BM-derived NSC-like cells exhibited some functional characteristics of developing neurons. Portions of the data were previously presented in abstracts.

Materials and Methods

Induction, culture, and expansion of NSC-like cells from hMeSCs

The hMeSCs from 4 donors were commercially obtained from AllCells LLC and Cambrex Bioscience. The cell lines were negative for surface markers associated with hematopoietic cells (eg, CD11b, CD33, CD34, and CD133) and retained their ability to differentiate along mesenchymal cell lineages. The NSC-like cells were induced from hMeSCs by culturing hMeSCs (1×10^5 cells/cm²) in T-75 tissue culture flasks containing CM collected from hNSC cultures at 37°C in a 5% CO₂ humidified incubation chamber (Fisher). The CM was prepared by culturing hNSCs for 2 weeks in a neurobasal medium (Gibco) containing B27 (1:50; Gibco), antibiotic–antimycotic mixture (1:100; Gibco), heparin (5 μ g/mL; Sigma), human recombinant epidermal growth factor (EGF, 20 ng/mL; R&D Systems), and human recombinant basic fibroblast growth factor (bFGF, 20 ng/mL; R&D Systems). The medium collected from the hNSCs, termed hNSC-CM, was centrifuged to remove cellular debris, and supernatant was filter sterilized with a 0.22- μ m membrane before use. Inspection of long-term (1 week) cultures confirmed that the hNSC-CM was cell free.

The hNSC-CM was changed every 2–3 days during the induction process, and cells were passaged after reaching about 80% of confluency. Cell aggregates formed 2–3 weeks

after the initial cultivation in hNSC-CM for all of the cell lines tested. Since these cell aggregates were morphologically similar to the spherical structures of cultured NSCs and the cells in the aggregates expressed molecular markers for NSCs, they were termed as NSC-like spheres and NSC-like cells, respectively.

These cellular aggregates were transferred into and expanded in uncoated tissue culture flasks (Falcon) containing a growth medium at 37°C in a 5% CO₂ humidified incubation chamber. The growth medium consisted of the neurobasal medium (Gibco) containing N2 supplement (1:100) or B27 (1:50; Gibco), penicillin (100 U/mL)/streptomycin (1 mg/mL; Gibco), heparin (5 μ g/mL; Sigma), human recombinant EGF (20 ng/mL; R&D Systems), human recombinant bFGF (20 ng/mL; R&D Systems), human recombinant leukemia inhibitory factor (10 ng/mL; Chemicon), human recombinant β -nerve growth factor (NGF, 10 ng/mL; R&D Systems), human recombinant brain-derived neurotrophic factor (BDNF, 25 ng/mL; R&D Systems), and human recombinant glial cell line–derived neurotrophic factor (10 ng/mL; R&D Systems). The medium was changed every 3–4 days by removing 50% of the medium and adding fresh medium.

Differentiation of NSC-like spheres

The terminal neural differentiation was induced by plating NSC-like spheres onto poly-L-lysine (Sigma)-coated coverslips and culturing in the differentiation medium for up to 14 days. The differentiation medium consisted of neurobasal medium containing N2 supplement (1:100) or B27 (1:50), penicillin (100 U/mL)/streptomycin (1 mg/mL), L-glutamine (2 mM), mouse laminin (1 μ g/mL; Invitrogen), BDNF (50 ng/mL), and NGF (10 ng/mL). The cultures were maintained in a 5% CO₂ humidified incubation chamber at 37°C and the medium was changed every 2–3 days.

Immunocytochemistry

After differentiation, cell samples were rinsed with 0.01 M phosphate-buffered saline (PBS) and fixed with 4% paraformaldehyde in PBS for 20 min at room temperature. Cells were washed in PBS and incubated in blocking buffer containing 0.1% Triton X-100 (Sigma) and 3% donkey serum (Jackson ImmunoResearch) in PBS for 30 min. Fluorescent immunocytochemical staining was performed by incubating the cells in primary antisera diluted in the blocking buffer overnight at 4°C. The primary antibodies used were mouse anti- β III-tubulin (1:600; Sigma), mouse anti-NF-200 (1:600; Chemicon), rabbit anti-glutamate (1:500; Sigma), and rabbit anti-GFAP (1:1,000; Abcam). Cells were then washed in PBS and incubated with corresponding secondary antibodies conjugated with rhodamine (tetramethylrhodamine isothiocyanate) or fluorescein (fluorescein isothiocyanate, 1:200; Jackson ImmunoResearch) for 2 h at room temperature in the dark. Finally, cells were washed in PBS, counterstained with 4',6-diamidino-2-phenylindole (Vector Labs), and viewed by immunofluorescence microscopy (Zeiss). Negative controls consisted of secondary antibodies application alone. Digitally captured images from fluorescence microscopy of stained cells were analyzed by NIH Image software (NIH) with Cell Scoring, Particle Analysis, and Cell Analysis macros.

Electrophysiological recording

Whole-cell patch-clamp recordings were performed on cells differentiated from the NSC-like cell aggregates after culturing in the differentiation medium for 2–13 days. Coverslips with differentiated cells were placed into a recording chamber and superfused with oxygenated (95% O₂ and 5% CO₂) artificial cerebrospinal fluid [aCSF: 122 mM NaCl, 3 mM potassium chloride (KCl), 0.81 mM MgSO₄, 2.5 mM CaCl₂, 1 mM NaH₂PO₄, 24 mM NaHCO₃, and 10 mM glucose, pH 7.4]. Patch pipettes (5–15 MΩ) were fabricated from borosilicate glass capillary tubing (outer diameter 1.5 mm; A-M Systems) using a Sutter Instruments P-97 micropipette puller (Novato). Patch pipettes were filled with 140 mM K-gluconate, 11 mM ethylenediaminetetraacetic acid, 1 mM CaCl₂, 10 mM 4-(2-hydroxyethyl)-1-piperazineethanesulfonic acid (HEPES), and 3.5 mM KOH. Cells differentiated from NSC-like cells with neuron-like morphology (a relatively rounded cell body with extended processes) were chosen for whole-cell patch-clamp recording as performed previously [26]. Physiological signals were amplified and low-pass filtered 10,000 Hz using a MultiClamp 700B (Axon Instruments). The data were digitized at a rate of 10,000 Hz (Digidata 1440A; Axon Instruments), and stored on a computer for later analysis (pClamp 10; Axon Instruments). The passive membrane properties of these cells, including the rest potential, input resistance, capacitance, and time constant, were determined by stimulating with 5 mV hyperpolarizing steps in voltage clamp. Active properties were investigated in current clamp by stimulating cells with a series of 400 ms current steps beginning at –100 pA and increasing to 300 pA in 50 pA intervals. All experiments were performed at room temperature.

Pharmacology of action potentials

The neuron-like cells were stimulated with a series of 7 current steps ranging from 0 to 300 pA in 50 pA intervals. Cells were stimulated once every minute and after the response stabilized, the inhibitors were applied through the perfusion system. Typically inhibitor applications lasted for 10 min and were followed by washes with aCSF. Drugs were dissolved in aCSF immediately before application. The voltage-gated sodium channel inhibitors [lidocaine hydrochloride and tetrodotoxin (TTX)] and voltage-gated calcium channel inhibitors (cadmium chloride and nickel chloride) were obtained from Sigma. We also used TTX from a second source (Biomol) in this experiment with similar results.

Calcium imaging

The responses of the neuron-like cells to 55 mM KCl and 100 μM L-glutamate were recorded using a calcium imaging system after culturing in the differentiation medium for 3–14 days. Cytosolic Ca²⁺ was monitored with ratiometric Ca²⁺ indicator, Fura-2. Coverslips with differentiated cells were washed twice in Hanks balanced salt solution (HBSS, 137 mM NaCl, 5.4 mM KCl, 0.25 mM Na₂HPO₄, 0.44 mM KH₂PO₄, 1.3 mM CaCl₂, 1.0 mM MgSO₄, and 4.2 mM NaHCO₃). After washing, the cells were incubated in 2 mL HBSS containing 5.0 μM Fura-2 AM and 0.066% Pluronic F-127 for 30–45 min at 37°C in the dark. Then, coverslips with the Fura-2-loaded cells were washed twice in HBSS to remove extracellular dye

and mounted in an imaging chamber containing Mg²⁺-free HBSS.

Fluorescence measurements were obtained at excitation wavelengths of 340 and 380 nm and emission at 510 nm on individual neuron-like cells using an inverted fluorescence microscope (Model IX-70; Olympus). The base-line intracellular Ca²⁺ levels were measured as a ratio of 340/380 nm fluorescence in individual cells incubated in Mg²⁺-free HBSS buffer. Cells were then exposed to 55 mM KCl or 100 μM L-glutamate. Typically, Ca²⁺ levels at rest or in response to challenges were measured simultaneously for 10–30 cells within a microscopic field, with 3–5 microscopic fields measured per condition. One microscopic field was measured in each Petri dish. Each cell was tested under only one condition. The amplitude of the drug-induced intracellular Ca²⁺ transient was determined for each cell by subtracting the base-line Ca²⁺ level from the drug-induced level.

Statistical analysis

Sample sizes for the calcium imaging experiments ranged from 30 to 50 cells for each of the different days in culture. Data were collected from at least 3 different trials. The within-group comparisons of the 340/380 ratio before and after the drug applications were performed using a single-tailed paired Student's *t*-test on the data from individual cells.

Results

Differentiation of BM-derived NSC-like cells

BM-derived NSC-like cells differentiated into neural cells, including glia and neurons, after culturing in the differentiation medium. We observed that the cells migrated from the neurosphere-like structures, attached to coverslips, and extended processes (Fig. 1). These morphological changes were concurrent with changes in protein expression patterns based on immunocytochemistry. Coverslips of differentiated NSC-like cells were stained with antisera directed against neuronal markers (βIII-tubulin, NF-200, or glutamate) and a glial marker (GFAP). Figure 1 shows that cells with neuron-like morphology (small rounded cell bodies and extended processes) were positively stained by antisera directed against neuronal markers, βIII-tubulin, NF-200, or glutamate. Analysis of the immunocytochemistry revealed that ~40% of the differentiated NSC-like cells expressed the immature neuronal marker βIII-tubulin. The neuron-like cells also expressed other neuronal markers, including doublecortin, MAP₂, and GABA (data not shown). Cells with glia-like morphologies (flat, polygonal, and star-like cell bodies) were positively stained with antisera directed against the glial marker GFAP (Fig. 1A). We found that ~60% of the total cells were labeled with the anti-GFAP antisera. At the beginning of the serum-free culture, a subpopulation of the undifferentiated hMeSCs expressed low levels of the neural progenitor marker nestin; however, we did not detect expression of the other neuronal markers in the undifferentiated hMeSCs by fluorescence immunocytology (data not shown). Because a subpopulation of cells differentiated from the BM-derived NSC-like cells had the morphology and protein expression patterns of neurons, we investigated the functional properties of these cells.

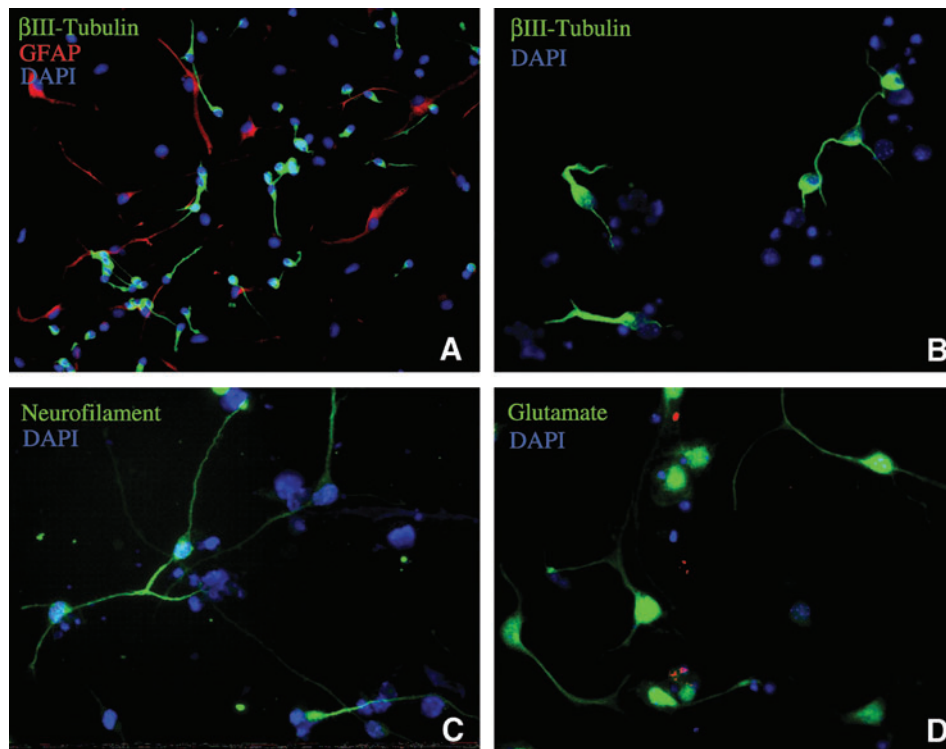


FIG. 1. Neural stem cell (NSC)-like cells derived from bone marrow differentiated into neuron and glia-like cells after 5 days in a defined culture medium. (**A, B**) NSC-like cells differentiated into cells with neuronal and glial morphology expressing β III-tubulin (**A, B**) and glial fibrillary acidic protein (GFAP) (**A**), respectively. (**C, D**) The differentiated neuron-like cells expressed the neuronal markers neurofilament 200 (**C**) and glutamate (**D**). Nuclei were labeled with the nucleic acid counterstain 4',6-diamidino-2-phenylindole (DAPI).

Neuron-like cells differentiated from BM-derived NSC-like cells have active membrane properties

We investigated whether the neuron-like cells with rounded cell bodies and extended processes differentiated from the NSC-like spheres had the electrophysiological properties of functional neurons. Whole-cell patch-clamp recordings were performed on >60 cells with this neuron-like morphology after growing in the differentiation medium for 2–13 days. The passive membrane properties of these cells, including the resting membrane potential, input resistance, capacitance, and time constant, were determined. We did not detect any obvious differences in the passive membrane properties at the ages tested. The resting membrane potentials for cells with a neuron-like morphology ranged from -25 to -58 mV with an average potential of -37.6 ± 1.3 mV (average \pm SEM, $N = 60$). The input resistance ranged from 0.2 to 8.3 G Ω with an average of 1.7 ± 0.2 G Ω ($N = 51$), the membrane capacitance ranged from 2.8 to 33.9 pF with an average of 12.1 ± 0.9 pF ($N = 51$), and the time constant ranged from 100 to $2,300$ μ s with an average of 593 ± 71 μ s ($N = 51$). The variation in the input resistance, membrane capacitance, and time constant indicated that the neuron-like cells had a wide range of different sizes and electrical characteristics. These results could indicate that the neuron-like cells were at different developmental stages or that the NSC-like spheres were capable of generating many distinct neuronal or glial subtypes.

The neuron-like cells were also subjected to a series of current pulses to determine if they were capable of generating depolarization-induced action potentials. We found that nearly all (98%) of the cells with neuron-like morphology exhibited active membrane properties in response to the depolarizing current pulses. The most common response was a single spike-like event early in the depolarizing current step (Fig. 2F). Representative examples of spike-like structures with overshoots and brief afterhyperpolarizations recorded from 2 different neurons are shown in Fig. 2A and B. The width of the spike-like structures was ~ 5 ms for both cells measured at 50% of the peak amplitude. Also notice that the steady-state voltage responses were rectifying for these 2 cells (Fig. 2A, B, and E), indicating the presence of voltage-gated potassium channels. The cells that did not generate overshooting spike-like events usually had smaller bumps without overshoot in the beginning of the depolarizing current steps and rectifying current–voltage relationships (Fig. 2C, E). These bumps were detected in 27% of the neuron-like cells. Only one cell completely lacked active membrane properties in response stimulation and was presumably a glia-like or undifferentiated cell (Fig. 2D, E).

The neuron-like cells often responded to the hyperpolarizing current steps with a rebound excitation that sometimes elicited a spike-like event. We detected postinhibitory rebound excitation in 37% of the neuron-like cells (26 of 70).

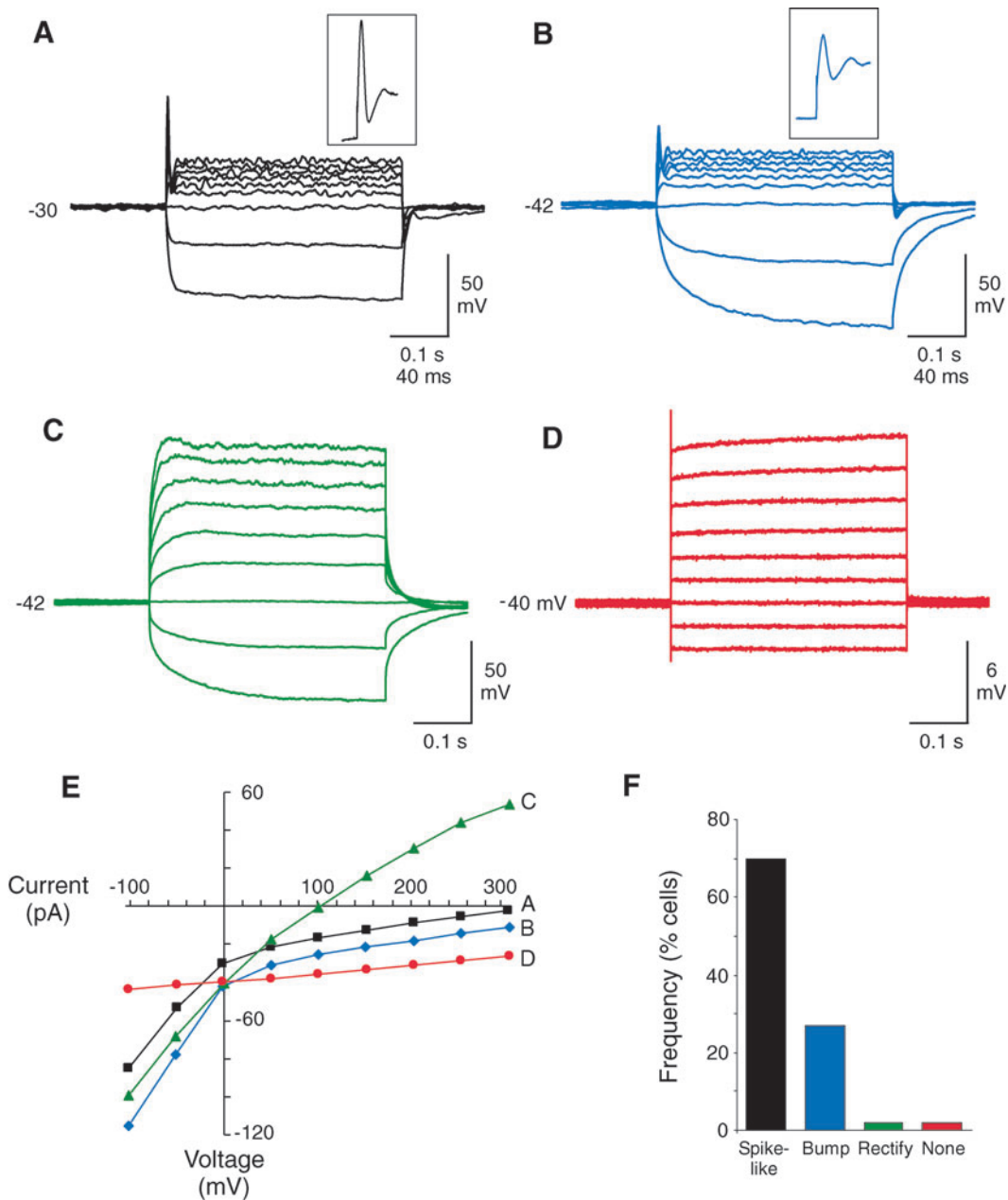


FIG. 2. Neuron-like membrane properties of neuron-like cells differentiated from human mesenchymal stem cell-derived neural stem cell-like cells. **(A–D)** Patch-clamp recordings showing the responses of 4 different cells to a series of current pulses. The cells in *panels A and B* had spike-like events with overshoot and afterhyperpolarizations at the beginning of the current steps. The cell in *panel C* had an active response without a spike-like event and the response of the cell in *panel D* was passive. Cells were stimulated with 400 ms current steps beginning at -100 pA and increasing to 300 pA in 50 pA intervals. Resting membrane potential (mV) is indicated to the left of the voltage recordings. **(E)** Plot of the steady-state current–voltage relationship for the cells in *panels A–D*. Notice that the plots were rectifying (nonlinear) for the cells in *panels A–C*, indicating an active voltage response. The cell in *panel D* had only a passive (linear) response. **(F)** Graph of the frequency of cells with active and passive responses to the current steps. A majority of the neuron-like cells generated spike-like structures with overshoots and brief afterhyperpolarizations.

The excitation triggered rebound spikes in 8 of these cells. Figure 3 shows current clamp records from a neuron-like cell that produced spikes to hyperpolarizing steps. Taken together, these data indicated that the BM-derived NSC-like spheres were capable of differentiating into cells that had the morphology, immunocytochemistry, and electrophysiological membrane properties associated with neurons.

Action potentials of the neuron-like cells are sodium dependent

The ionic properties of the spike-like events were investigated using inhibitors of voltage-gated sodium and calcium channels. The neuron-like cells were depolarized with a series of current steps, and, after the response stabilized, the

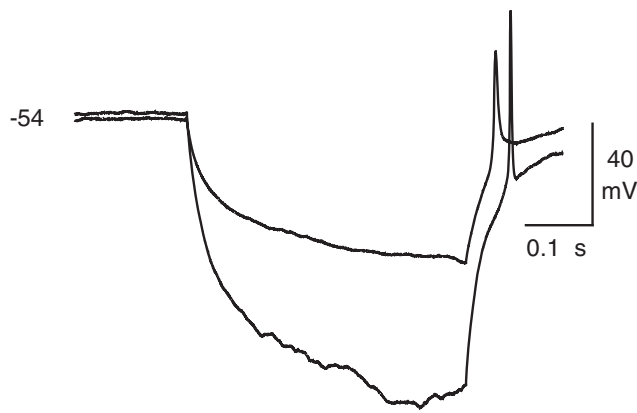


FIG. 3. Rebound from hyperpolarization induces action potentials in neuron-like cells differentiated from neural stem cell-like cells. Patch clamp recording showing the rebound excitation and subsequent spike-like events after -100 and -50 pA hyperpolarizing current steps (400 ms). Resting membrane potential (mV) is indicated to the left of the voltage recordings.

inhibitors were applied through the perfusion system. We found that the spike-like events were blocked by the voltage-gated sodium channel inhibitor lidocaine (3.5 mM, $N = 4$; Fig. 4A). In contrast, another sodium channel inhibitor TTX did not block the action potentials of any of the tested cells (1 μ M TTX, $N = 5$; 10 μ M TTX, $N = 5$; Fig. 4B). These experiments were performed using TTX from 2 different sources with the same results. Next we tested whether calcium ions contributed to the spike-like events using 2 voltage-gated calcium channels inhibitors, nickel and cadmium. The application of

1 mM nickel ($N = 2$) or 10 μ M cadmium ($N = 2$) did not block the depolarization-evoked spikes (Fig. 5). We did, however, observe slight changes in the action potential shape and more pronounced changes in the amplitude of the steady-state depolarization, suggesting that there was calcium influx during the depolarization and that calcium may modulate the process of repolarization. These data indicated that the neuron-like cells express TTX-resistant voltage-gated sodium channels that are capable of generating sodium-dependent action potentials.

Neuron-like cells differentiated from BM-derived NSC-like cells respond to the neurotransmitter L-glutamate

In addition to sodium and potassium channels, functional neurons express calcium channels that are activated by depolarization and receptors for fast-acting neurotransmitters. We used a calcium imaging system to investigate whether the neuron-like cells derived from the BM expressed voltage-gated calcium channels and if they expressed receptors that respond to L-glutamate, a neurotransmitter that is commonly used in the CNS. The advantage of this technique is that it permits large number of cells to be rapidly screened compared to patch clamping. The neuron-like cells were loaded with a ratiometric Ca^{2+} indicator, Fura-2, and the cytosolic Ca^{2+} level was monitored while the cells were exposed to KCl or L-glutamate. KCl depolarizes cells and increases Ca^{2+} influx by activating voltage-gated calcium channels. L-Glutamate increases Ca^{2+} levels by directly activating receptors that are permeable to Ca^{2+} ions. We observed that both KCl and L-glutamate stimulated a relatively rapid rise in the intracellular Ca^{2+} concentration in most of the neuron-like

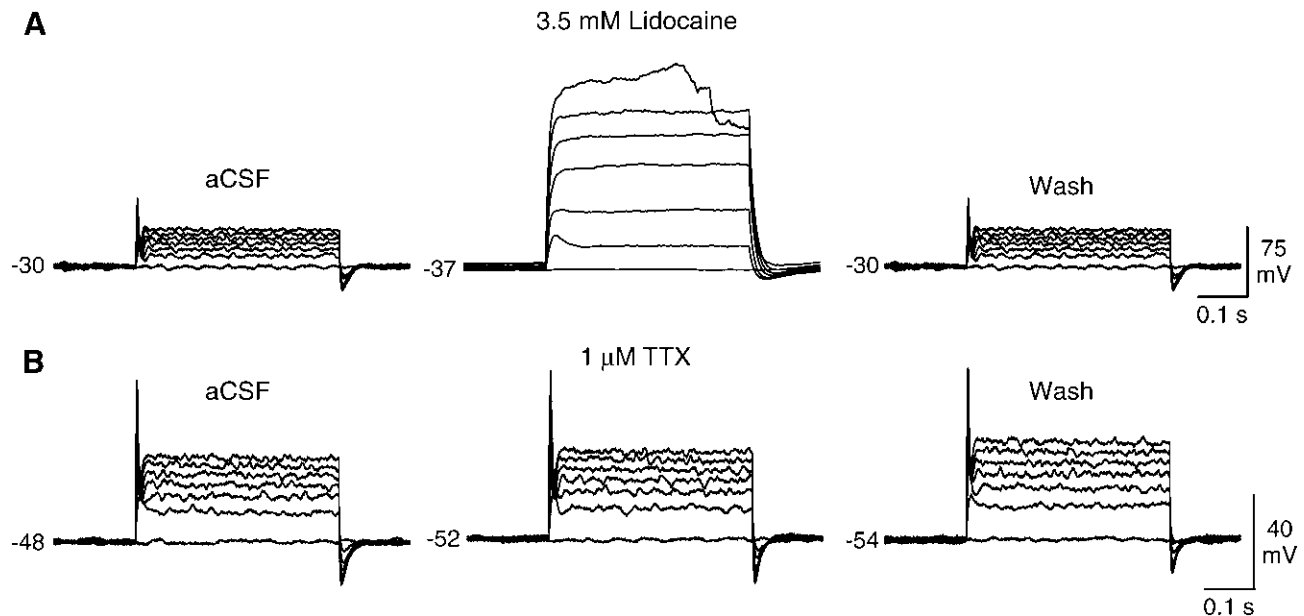


FIG. 4. Effects of sodium channel inhibitors on depolarization-induced action potentials in neuron-like cells differentiated from neural stem cell-like cells. **(A)** The depolarization-induced action potentials were inhibited by 3.5 mM lidocaine. Notice that the inhibition reversed after washing with control saline [(artificial cerebrospinal fluid (aCSF))]. **(B)** Tetrodotoxin (TTX, 1 μ M) had little effect on the action potential or the steady-state currents, suggesting that the spikes are generated by TTX-resistant voltage-gated sodium channels. Resting membrane potential (mV) is indicated to the left of the voltage recordings. Recordings are representative examples.

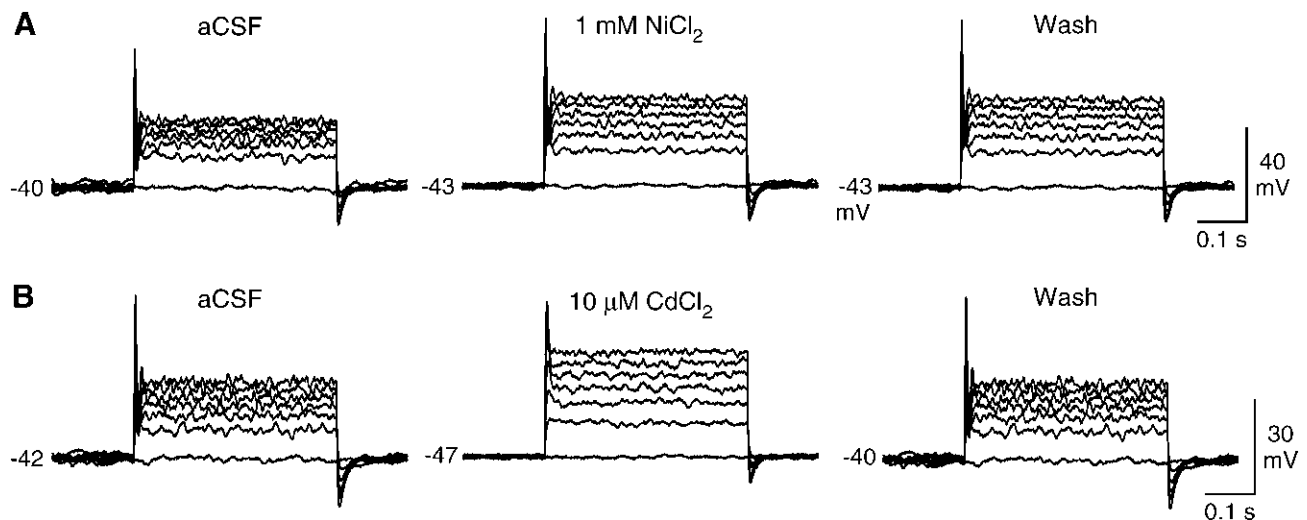


FIG. 5. Effects of calcium channel inhibitors on depolarization-induced action potentials in neuron-like cells differentiated from neural stem cell-like cells. **(A)** The depolarization-induced action potentials were not affected by 1 mM nickel chloride (NiCl₂). However, the amplitude of the steady-state depolarization changed. **(B)** The action potential shape and the steady-state depolarization were altered by 10 μM cadmium chloride (CdCl₂). Resting membrane potential (mV) is indicated to the left of the voltage recordings. Recordings are representative examples.

cells (Fig. 6). KCl (55 mM) elicited an increase in the intracellular Ca²⁺ level in 92% of the tested cells and L-glutamate (100 μM) elicited an increase in 87% of the cells.

We also examined if the length of time in culture affected the amplitude of the KCl- and L-glutamate-induced Ca²⁺ signals. Cells were exposed to either KCl or L-glutamate after culturing in the differentiation medium for 3–14 days. We observed that the responses of the neuron-like cells gradually developed with time in the differentiation medium. Initially, the application of KCl and L-glutamate did not significantly increase the cytoplasmic Ca²⁺ levels in the neuron-like cells (Fig. 6A). However, after 4 days in the differentiation medium, the KCl-induced Ca²⁺ signals began to increase reaching a maximum on day 7. The L-glutamate-induced signals took longer to develop, increasing significantly after 6 days in culture and peaking on day 9 (Fig. 6B). The calcium imaging suggests that the neuron-like cells express some of the components necessary for synaptic transmission because KCl and L-glutamate induced increases in the cytosolic Ca²⁺ level, presumably by activating voltage-gated calcium channels and glutamate receptors, respectively.

Discussion

Here we report that human BM-derived NSC-like cells differentiated into cells with the morphology and some of the functional properties of neurons. Patch clamp experiments demonstrated that the neuron-like cells were capable of generating action potentials and expressed TTX-resistant sodium channels. Calcium imaging revealed depolarization- and L-glutamate-evoked increases in the cytoplasmic Ca²⁺ levels, indicating that there were functional voltage-gated calcium channels and L-glutamate receptors. Therefore, the neuron-like cells expressed components of the machinery used to conduct action potentials, initiate neurotransmitter release, and respond to a released transmitter. All of these functions of neuron-like cells were induced using a defined

culture system containing hNSCs-CM without harsh chemicals, cell cocultures, or genetic manipulations.

Membrane properties of neuron-like cells differentiated from BM-derived NSC-like cells

For years, scientists have known how to grow human embryonic and adult NSCs in culture and differentiate them into mature neurons capable of TTX-sensitive depolarization-dependent action potentials [27,28]. In spite of this, ethical issues and the limited availability of embryo- and brain-derived stem cells have curbed their clinical usefulness. Here we have shown that stem cells from an easily accessible tissue, adult human BM, can be converted in culture into NSC-like cells capable of differentiating into cells with multiple functional characteristics of neurons. This culture system may be capable of generating large quantities of NSCs or immature neurons suitable for neuroreplacement therapy.

Initially, we examined the passive properties of the neuron-like cells differentiated from the BM-derived NSC-like cells and found them to be highly variable. This variation indicated that the neuron-like cells had a wide range of different sizes and/or electrical characteristics that could reflect differences in their developmental stages or the types of neurons being generated. The passive membrane properties of the neuron-like cells were similar to previously published data for neurons differentiated from human and rodent embryonic stem cells [27,29], human and rodent NSCs [28,30–32], and rodent MeSCs [33]. Although the passive properties revealed that the NSC-like cells might have differentiated into a diverse population of neuron-like cells, it did not indicate anything about their functional characteristics. To examine function we tested whether the neuron-like cells could generate action potentials, express voltage-gated calcium channels, or respond to the neurotransmitter L-glutamate.

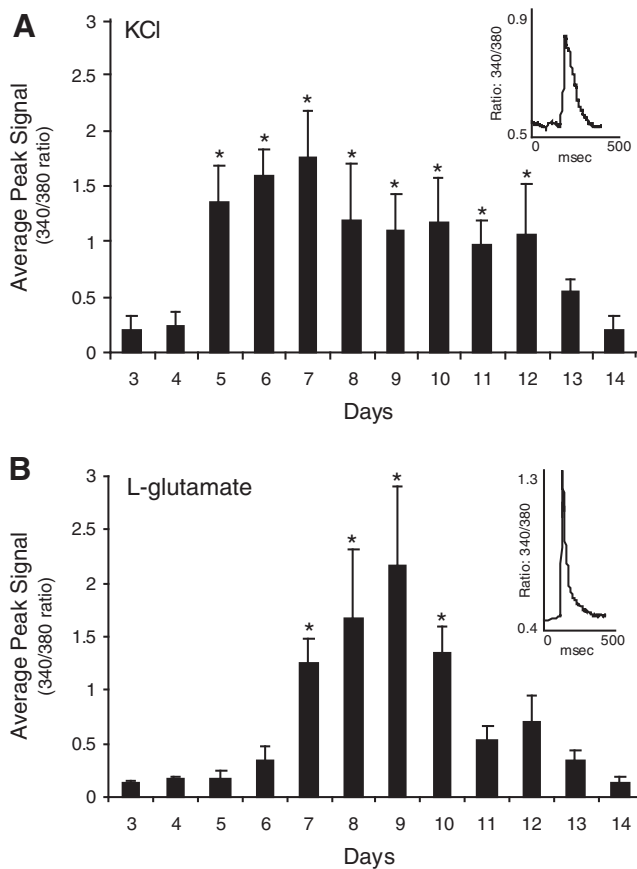


FIG. 6. Potassium chloride (KCl) and L-glutamate increase the intracellular calcium levels of the neuron-like cells differentiated from neural stem cell-like spheres. **(A)** Time course of the average peak calcium signal recorded from neuron-like cells after the application of 55 mM potassium. The neuron-like cells developed the capability to respond to potassium on the fifth day in culture and the response peaked on day 7. **(B)** Time course of the average peak calcium signal recorded from neuron-like cells after the application of 100 μ M L-glutamate. The neuron-like cells developed the capability to respond to L-glutamate on the seventh day in culture and the response peaked on day 9. Insets show the average response of the cells from a single experiment. Asterisks indicate that the average peak 340/380 ratio was significantly different from the baseline before the KCl or L-glutamate application ($P < 0.001$, Student's paired *t*-test).

One important function of neurons is the ability to generate and conduct action potentials. We used patch clamp recordings to show that the BM-derived neuron-like cells were capable of generating action potentials in response to depolarizing current steps. Some of the cells were also capable of responding to hyperpolarizing current with a rebound excitation and spike. A majority of the action potentials that we detected had small overshoots and brief afterhyperpolarizations. The shape of the action potentials recorded from the neuron-like cells resembled the immature action potentials that are commonly observed for developing human neurons [26] and neuron-like cells differentiating from stem cells isolated from both humans [14,25,28,30] or from rodents [29,32,33]. In addition, the patch clamp re-

cordings were atypical for mature neurons in that the spikes were not blocked by the sodium channel inhibitor TTX at concentrations up to 10 μ M, and we did not observe any repetitive spikes or spontaneous action potentials. The action potentials were blocked by another voltage-gated sodium channel inhibitor lidocaine (Fig. 4A). On the basis of the electrophysiological properties of the neuron-like cells, we believe that our data demonstrate that hMeSCs derived from adult BM were clearly reprogrammed and directed toward a neuronal lineage. Recent voltage clamp studies have shown that a subset of undifferentiated hMeSCs, isolated from either the BM or amniotic fluid, express the ion channels necessary to generate action potentials [34–36]. However, the density of the voltage-gated sodium channels is very low compared to mature neurons, suggesting that the undifferentiated hMeSCs are incapable of producing action potentials. Attempts to induce action potentials in hMeSCs using depolarizing current pulses have confirmed that undifferentiated MeSCs isolated from the adult BM of humans or rodents do not generate action potentials [14,21,25,37–40].

It is also possible that some of the action potentials we recorded were from cells other than neurons because astrocytes and oligodendrocytes express many of the voltage-gated ion channels found in neurons and can produce action potentials [41–43]. However, there are several reasons that we believe that most of the neuron-like cells were indeed neurons. First, the neuron-like cells used in this study were smaller than typical astrocytes. We used the membrane capacitance as an approximate measure of cell size and found that the average capacitance of the neuron-like cells (~ 12 pF) was smaller than the capacitance reported for human and rat brain astrocytes (30–80 pF) [41–44]. Second, the prevalence of the spike-like events with overshoot and afterhyperpolarization is higher than would be expected for glial cells. Normally, the sodium current is much smaller than the potassium current in astrocytes and they rarely fire action potentials [45,46]. Besides, similar immature action potentials and current–voltage relationships are often observed for developing human neurons [26] and neuron-like cells differentiated from stem cells isolated from humans [14,25,28,30,37,47,48] or from rodents [29,32,33,49,50]. Finally, consistent with those previously published studies [9,11–14,25,47,48,51–54], we confirmed that neuron-like cells with neuronal morphology usually express neuronal and not glial markers (Fig. 1A). Taken together, our results strongly suggest that the NSC-like cells derived from adult BM hMeSCs were capable of developing into cells with the electrophysiological properties of immature neurons.

Development of KCl and L-glutamate-induced increases in cytoplasmic calcium levels

Previous calcium imaging studies have shown that cells differentiated from adult MeSCs, adult NSCs, and embryonic stem cells respond to depolarization with KCl or the application of the neurotransmitter L-glutamate with an increase in cytoplasmic Ca^{2+} levels [27,31,38,55,56]. These transient changes in the Ca^{2+} levels are important for regulating neuronal differentiation, transmitter selection, and axonal targeting in immature neurons [57,58]. After maturation, calcium signals regulate multiple cellular processes, such as the cell viability, gene transcription, and synaptic transmis-

sion [59,60]. Using calcium imaging, we observed that the neuron-like cells produced transient increases in the cytoplasmic Ca^{2+} levels in response to KCl and L-glutamate application. The KCl-evoked increase in the cytosolic Ca^{2+} levels was probably caused by a depolarization-dependent opening of voltage-gated calcium channels [61]. The L-glutamate-induced increase in Ca^{2+} could be caused by a direct influx of extracellular Ca^{2+} through glutamate receptor ion channels or an indirect influx through voltage-gated calcium channels after the glutamate-evoked depolarization [62]. Our calcium imaging experiments extend the previous studies and demonstrate that the BM-derived NSC-like cells were capable of differentiating into cells that had many of the basic functional properties of neurons in our defined culture system.

Typically, the differentiation of embryonic stem cells, *in vivo* and *in vitro*, is a gradual process regulated by both genetic factors and microenvironmental cues [63–66]. We found that the differentiation and maturation of the BM-derived NSC-like cells were also gradual processes with each of the neuron-like characteristics developing after different lengths of time in culture. It took only 2–3 days in the differentiation medium for the neuron-like cells to exhibit action potentials in response to a depolarizing current steps, whereas functional expression of voltage-gated calcium channels increased significantly on day 5 and the L-glutamate-evoked increase in the Ca^{2+} signal began on day 7 (Fig. 6). It is important to note that we did not observe any repetitive spikes or spontaneous action potentials in these neuron-like cells, implying that even after 13 days in culture, these cells were not fully developed neurons [67]. This is similar to the time course for the differentiation of both multipotent progenitor cells isolated from adults and embryonic stem cells. Multipotent progenitor cells isolated from human or mouse brains [30,32] or mouse embryonic stem cells [50] do not usually express mature action potentials until they are cultured >2 weeks. This gradual development is consistent with the immunocytochemical analysis of neuronal differentiation markers under similar culture conditions. The differentiating NSC-like cells began to express a marker for immature neurons, β III-tubulin, after 3–5 days, and with increasing the time in culture, they increased expression of a marker for more mature neurons, MAP₂.

Conclusions

Cells derived from human BM were induced in culture to express proteins that are considered markers of neuronal and glial differentiation. More importantly, the neuron-like cells expressed functionally active voltage- and ligand-gated ion channels. These cells appeared to be neuronal precursor cells or immature neurons at different stages in development, although it is possible that the BM-derived NSC-like cells will develop into mature neurons with increased time for *in vitro* differentiation or in a more appropriate environment for differentiation such as transplantation into the brain. Our results, in combination with previous studies by others, suggest that there are many different ways to trigger hMeSCs to transform into neuron-like cells *in vitro*. The future challenge will be to identify the culture conditions necessary to generate specific neuronal cell types that will function properly and integrate into the CNS after trans-

plantation. Transplantation of individual patients' BM-derived autologous NSC-like cells for neuroreplacement therapy would have the advantage of avoiding some controversial ethical issues and the risk of immune rejection.

Acknowledgments

This work was supported by grants NINDS R01 NS052372 to Dr. Jianguo Cheng, and the Charles H. and Bertha L. Boothroyd Foundation and American Health Assistance Foundation (AHAF) grants to Tingyu Qu.

Author Disclosure Statement

None of the authors, Lyle E. Fox, Jun Shen, Ke Ma, Qing Liu, Guangbin Shi, George D. Pappas, Tingyu Qu, or Jianguo Cheng, or their immediate families have any actual or potential commercial associations that might create a conflict of interest in connection with this article.

References

- Li JY, NS Christophersen, V Hall, D Soulet and P Brundin. (2008). Critical issues of clinical human embryonic stem cell therapy for brain repair. *Trends Neurosci* 31:146–153.
- Mathews DJ, J Sugarman, H Bok, DM Blass, JT Coyle, P Duggan, J Finkel, HT Greely, A Hillis, A Hoke, R Johnson, M Johnston, J Kahn, D Kerr, J Kurtzberg, SM Liao, JW McDonald, G McKhann, KB Nelson, M Rao, A Regenberg, AW Siegel, K Smith, D Solter, H Song, A Vescovi, W Young, JD Gearhart and R Faden. (2008). Cell-based interventions for neurologic conditions: ethical challenges for early human trials. *Neurology* 71:288–293.
- Erdö F, C Bührle, J Blunk, M Hoehn, Y Xia, B Fleischmann, M Föcking, E Küstermann, E Kolossov, J Hescheler, KA Hossmann and T Trapp. (2003). Host-dependent tumorigenesis of embryonic stem cell transplantation in experimental stroke. *J Cereb Blood Flow Metab* 23:780–785.
- Rubio D, J Garcia-Castro, MC Martín, R de la Fuente, JC Cigudosa, AC Lloyd and A Bernad. (2005). Spontaneous human adult stem cell transformation. *Cancer Res* 65:3035–3039.
- Nussbaum J, E Minami, MA Laflamme, JA Virag, CB Ware, A Masino, V Muskheli, L Pabon, H Reinecke and CE Murry. (2007). Transplantation of undifferentiated murine embryonic stem cells in the heart: teratoma formation and immune response. *FASEB J* 21:1345–1357.
- Bianco P, M Riminucci, S Gronthos and PG Robey. (2001). Bone marrow stromal stem cells: nature, biology, and potential applications. *Stem Cells* 19:180–192.
- Reyes M, T Lund, T Lenvik, D Aguiar, L Koodie and CM Verfaillie. (2001). Purification and *ex vivo* expansion of postnatal human marrow mesodermal progenitor cells. *Blood* 98:2615–2625.
- Sekiya I, BL Larson, JR Smith, R Pochampally, JG Cui and DJ Prockop. (2002). Expansion of human adult stem cells from bone marrow stroma: conditions that maximize the yields of early progenitors and evaluate their quality. *Stem Cells* 20:530–541.
- Sanchez-Ramos J, S Song, F Cardozo-Pelaez, C Hazzi, T Stedeford, A Willing, TB Freeman, S Saporta, W Janssen, N Patel, DR Cooper and PR Sanberg. (2000). Adult bone marrow stromal cells differentiate into neural cells *in vitro*. *Exp Neurol* 164:247–256.

10. Woodbury D, EJ Schwarz, DJ Prockop and IB Black. (2000). Adult rat and human bone marrow stromal cells differentiate into neurons. *J Neurosci Res* 61:364–370.
11. Black IB and D Woodbury. (2001). Adult rat and human bone marrow stromal stem cells differentiate into neurons. *Blood Cells Mol Dis* 27:632–636.
12. Deng W, M Obrocka, I Fischer and DJ Prockop. (2001). *In vitro* differentiation of human marrow stromal cells into early progenitors of neural cells by conditions that increase intracellular cyclic AMP. *Biochem Biophys Res Commun* 282:148–152.
13. Lee J, AG Elkhoulou, SA Messina, N Ferrari, D Xi, CL Smith, R Cooper, PS Albert and HA Fine. (2003). Cellular and genetic characterization of human adult bone marrow-derived neural stem-like cells: a potential anti-glioma cellular vector. *Cancer Res* 63:8877–8889.
14. Hermann A, R Gastl, S Liebau, MO Popa, J Fiedler, BO Boehm, M Maisel, H Lerche, J Schwarz, R Brenner and A Storch. (2004). Efficient generation of neural stem cell-like cells from adult human bone marrow stromal cells. *J Cell Sci* 117:4411–4422.
15. Qu TY, XJ Dong, I Sugaya, A Vaghani, J Pulido and K Sugaya. (2004). Bromodeoxyuridine increases multipotency of human bone marrow-derived stem cells. *Restor Neurol Neurosci* 22:459–468.
16. Bossolasco P, L Cova, C Calzarossa, SG Rimoldi, C Borsotti, GL Delilieri, V Silani, D Soligo and E Polli. (2005). Neuro-glial differentiation of human bone marrow stem cells *in vitro*. *Exp Neurol* 193:312–325.
17. Mezey E, S Key, G Vogelsang, I Szalayova, GD Lange and B Crain. (2003). Transplanted bone marrow generates new neurons in human brains. *Proc Natl Acad Sci USA* 100:1364–1369.
18. Weimann JM, CA Charlton, TR Brazelton, RC Hackman and HM Blau. (2003). Contribution of transplanted bone marrow cells to Purkinje neurons in human adult brains. *Proc Natl Acad Sci USA* 100:2088–2093.
19. Björklund A and O Lindvall. (2000). Cell replacement therapies for central nervous system disorders. *Nat Neurosci* 3:537–544.
20. Mahmood A, D Lu, L Yi, JL Chen and M Chopp. (2001). Intracranial bone marrow transplantation after traumatic brain injury improving functional outcome in adult rats. *J Neurosurg* 94:589–595.
21. Hofstetter CP, EJ Schwarz, D Hess, J Widenfalk, A El Manira, DJ Prockop and L Olson. (2002). Marrow stromal cells form guiding strands in the injured spinal cord and promote recovery. *Proc Natl Acad Sci USA* 99:2199–2204.
22. Zhao LR, WM Duan, M Reyes, CD Keene, CM Verfaillie and WC Low. (2002). Human bone marrow stem cells exhibit neural phenotypes and ameliorate neurological deficits after grafting into the ischemic brain of rats. *Exp Neurol* 174: 11–20.
23. Grove JE, E Bruscia and DS Krause. (2004). Plasticity of bone marrow-derived stem cells. *Stem Cells* 22:487–500.
24. Suzuki H, T Taguchi, H Tanaka, H Kataoka, Z Li, K Muramatsu, T Gondo and S Kawai. (2004). Neurospheres induced from bone marrow stromal cells are multipotent for differentiation into neuron, astrocyte, and oligodendrocyte phenotypes. *Biochem Biophys Res Commun* 322:918–922.
25. Fu L, L Zhu, Y Huang, TD Lee, SJ Forman and CC Shih. (2008). Derivation of neural stem cells from mesenchymal stem cells: evidence for a bipotential stem cell population. *Stem Cells Dev* 17:1109–1121.
26. Cheng J, A Nath, B Knudsen, S Hochman, JD Geiger, M Ma and DS Magnuson. (1998). Neuronal excitatory properties of human immunodeficiency virus type 1 Tat protein. *Neuroscience* 82:97–106.
27. Carpenter MK, MS Inokuma, J Denham, T Mujtaba, CP Chiu and MS Rao. (2001). Enrichment of neurons and neural precursors from human embryonic stem cells. *Exp Neurol* 172:383–397.
28. Westerlund U, MC Moe, M Varghese, J Berg-Johnsen, M Ohlsson, IA Langmoen and M Svensson. (2003). Stem cells from the adult human brain develop into functional neurons in culture. *Exp Cell Res* 289:378–383.
29. Ban J, P Bonifazi, G Pinato, FD Broccard, L Studer, V Torre and ME Ruaro. (2007). Embryonic stem cell-derived neurons form functional networks *in vitro*. *Stem Cells* 25:738–749.
30. Moe MC, M Varghese, AI Danilov, U Westerlund, J Ramm-Petersen, L Brundin, M Svensson, J Berg-Johnsen and IA Langmoen. (2005). Multipotent progenitor cells from the adult human brain: neurophysiological differentiation to mature neurons. *Brain* 128:2189–2199.
31. Moe MC, U Westerlund, M Varghese, J Berg-Johnsen, M Svensson and IA Langmoen. (2005). Development of neuronal networks from single stem cells harvested from the adult human brain. *Neurosurgery* 56:1182–1188.
32. Scheffler B, NM Walton, DD Lin, AK Goetz, G Enikolopov, SN Roper and DA Steindler. (2005). Phenotypic and functional characterization of adult brain neurogenesis. *Proc Natl Acad Sci USA* 102:9353–9358.
33. Jiang Y, D Henderson, M Blackstad, A Chen, RF Miller and CM Verfaillie. (2003). Neuroectodermal differentiation from mouse multipotent adult progenitor cells. *Proc Natl Acad Sci USA* 100 Suppl 1:11854–11860.
34. Heubach JF, EM Graf, J Leutheuser, M Bock, B Balana, I Zahanich, T Christ, S Boxberger, E Wettwer and U Ravens. (2003). Electrophysiological properties of human mesenchymal stem cells. *J Physiol* 554:659–672.
35. Li GR, H Sun, X Deng and CP Lau. (2005). Characterization of ionic currents in human mesenchymal stem cells from bone marrow. *Stem Cells* 23:371–382.
36. Mareschi K, D Rustichelli, V Comunanza, R De Fazio, C Cravero, G Morterra, B Martinoglio, E Medico, E Carbone, C Benedetto and F Fagioli. (2009). Multipotent mesenchymal stem cells from amniotic fluid originate neural precursors with functional voltage-gated sodium channels. *Cytotherapy* 11:534–547.
37. Cho T, JH Bae, HB Choi, SS Kim, JG McLarnon, H Suh-Kim, SU Kim and CK Min. (2002). Human neural stem cells: electrophysiological properties of voltage-gated ion channels. *Neuroreport* 13:1447–1452.
38. Hung SC, H Cheng, CY Pan, MJ Tsai, LS Kao and HL Ma. (2002). *In vitro* differentiation of size sieved stem cells into electrically active neural cells. *Stem Cells* 20:522–529.
39. Lu P and MH Tuszynski. (2005). Can bone marrow-derived stem cells differentiate into functional neurons? *Exp Neurol* 193:273–278.
40. Mareschi K, M Novara, D Rustichelli, I Ferrero, D Guido, E Carbone, E Medico, E Madon, A Vercelli and F Fagioli. (2006). Neural differentiation of human mesenchymal stem cells: evidence for expression of human markers and eag K⁺ channel types. *Exp Hematol* 34:1563–1572.
41. Barres BA, LL Chun and DP Corey. (1988). Ion channel expression by white matter glia: I. Type 2 astrocytes and oligodendrocytes. *Glia* 1:10–30.

42. Barres BA, LL Chun and DP Corey. (1989). Glial and neuronal forms of the voltage-dependent sodium channel: characteristics and cell-type distribution. *Neuron* 2:1375–1388.
43. Bordey A and H Sontheimer. (2000). Ion channel expression by astrocytes in situ: comparison of different CNS regions. *Glia* 30:27–38.
44. Bordey A and H Sontheimer. (1998). Properties of human glial cells associated with epileptic seizure foci. *Epilepsy Res* 32:286–303.
45. Barres BA. (1991). Glial ion channels. *Curr Opin Neurobiol* 1:354–359.
46. Sontheimer H. (1994). Voltage-dependent ion channels in glial cells. *Glia* 11:156–172.
47. Cho KJ, KA Trzaska, SJ Greco, J McArdle, FS Wang, JH Ye and P Rameshwar. (2005). Neurons derived from human mesenchymal stem cells show synaptic transmission and can be induced to produce the neurotransmitter substance P by interleukin-1 alpha. *Stem Cells* 23:383–391.
48. Greco SJ, C Zhou, JH Ye and P Rameshwar. (2007). An interdisciplinary approach and characterization of neuronal cells transdifferentiated from human mesenchymal stem cells. *Stem Cells Dev* 16:811–826.
49. Song HJ, CF Stevens and FH Gage. (2002). Neural stem cells from adult hippocampus develop essential properties of functional CNS neurons. *Nat Neurosci* 5:438–445.
50. Bibel M, J Richter, K Schrenk, KL Tucker, V Staiger, M Korte, M Goetz and YA Barde. (2004). Differentiation of mouse embryonic stem cells into a defined neuronal lineage. *Nat Neurosci* 7:1003–1009.
51. Tao H, R Rao and DD Ma. (2005). Cytokine-induced stable neuronal differentiation of human bone marrow mesenchymal stem cells in a serum/feeder cell-free condition. *Dev Growth Differ* 47:423–433.
52. Choi CB, YK Cho, KV Prakash, BK Jee, CW Han, YK Paik, HY Kim, KH Lee, N Chung and HK Rha. (2006). Analysis of neuron-like differentiation of human bone marrow mesenchymal stem cells. *Biochem Biophys Res Commun* 350:138–146.
53. Wensch S, K Trinkaus, A Hild, D Hose, C Heiss, V Alt, C Klisch, H Meissl and R Schnettler. (2006). Immunochemical, ultrastructural and electrophysiological investigations of bone-derived stem cells in the course of neuronal differentiation. *Bone* 38:911–921.
54. Yang Y, Y Li, Y Lv, S Zhang, L Chen, C Bai, X Nan, W Yue and X Pei. (2008). NRSF silencing induces neuronal differentiation of human mesenchymal stem cells. *Exp Cell Res* 314:2257–2265.
55. Kohyama J, H Abe, T Shimazaki, A Koizumi, K Nakashima, S Gojo, T Taga, H Okano, J Hata and A Umezawa. (2001). Brain from bone: efficient “meta-differentiation” of marrow stroma-derived mature osteoblasts to neurons with Noggin or a demethylating agent. *Differentiation* 68:235–244.
56. Deisseroth K, S Singla, H Toda, M Monje, TD Palmer and RC Malenka. (2004). Excitation-neurogenesis coupling in adult neural stem/progenitor cells. *Neuron* 42:535–552.
57. Spitzer NC. (2006). Electrical activity in early neuronal development. *Nature* 444:707–712.
58. Spitzer NC, PA Kingston, TJ Manning and MW Conklin. (2002). Outside and in: development of neuronal excitability. *Curr Opin Neurobiol* 12:315–323.
59. Catterall WA and AP Few. (2008). Calcium channel regulation and presynaptic plasticity. *Neuron* 59:882–901.
60. Neher E and T Sakaba. (2008). Multiple roles of calcium ions in the regulation of neurotransmitter release. *Neuron* 59:861–872.
61. Magee J, D Hoffman, C Colbert and D Johnston. (1998). Electrical and calcium signaling in dendrites of hippocampal pyramidal neurons. *Annu Rev Physiol* 60:327–346.
62. Reichling DB and AB MacDermott. (1993). Brief calcium transients evoked by glutamate receptor agonists in rat dorsal horn neurons: fast kinetics and mechanisms. *J Physiol* 469:67–88.
63. Lee SH, N Lumelsky, L Studer, JM Auerbach and RD McKay. (2000). Efficient generation of midbrain and hindbrain neurons from mouse embryonic stem cells. *Nat Biotechnol* 18:675–679.
64. Cai J, Y Wu, T Mirua, JL Pierce, MT Lucero, KH Albertine, GJ Spangrude and MS Rao. (2002). Properties of a fetal multipotent neural stem cell (NEP cell). *Dev Biol* 251:221–240.
65. Kintner C. (2002). Neurogenesis in embryos and in adult neural stem cells. *J Neurosci* 22:639–643.
66. Ying QL, M Stavridis, D Griffiths, M Li and A Smith. (2003). Conversion of embryonic stem cells into neuroectodermal precursors in adherent monoculture. *Nat Biotechnol* 21:183–186.
67. Zhang S, M Werning, ID Duncan, O Brustle and JA Thomson. (2001). *In vitro* differentiation of transplantable neural precursors from human embryonic stem cells. *Nat Biotechnol* 19:1129–1133.

Address correspondence to:

Dr. Jianguo Cheng
Department of Pain Management
The Cleveland Clinic Foundation
9500 Euclid Avenue
Cleveland, OH 44195

E-mail: chengj@ccf.org

Dr. Tingyu Qu
Department of Psychiatry
The Psychiatric Institute
College of Medicine
University of Illinois at Chicago (UIC)
1601 West Taylor Street
Chicago, IL 60612

E-mail: tq@uic.edu

Received for publication February 21, 2010

Accepted after revision April 15, 2010

Prepublished on Liebert Instant Online April 15, 2010

